Journal of Power Sources 199 (2012) 355–359

Contents lists available at SciVerse ScienceDirect

Journal of Power Sources

journal homepage: www.elsevier.com/locate/jpowsour

Short communication

A high capacity cathode material-MnO_2 doped with nano $Ag_4Bi_2O_5$ for alkaline secondary batteries

Qian Wang [a], Junqing Pan [a,*], Yanzhi Sun [b,**], Zihao Wang [a]

[a] State Key Laboratory of Chemical Resource Engineering, Beijing University of Chemical Technology, Beijing 100029, China
[b] National Fundamental Research Laboratory of New Hazardous Chemicals Assessment and Accident Analysis, Beijing University of Chemical Technology, Beijing 100029, China

ARTICLE INFO

Article history:
Received 15 June 2011
Received in revised form 27 August 2011
Accepted 17 October 2011
Available online 20 October 2011

Keywords:
Manganese dioxide
Silver bismuthates
Doped electrode
Specific discharge capacity

ABSTRACT

In the present paper, we report a novel MnO_2 cathode material doped with nano $Ag_4Bi_2O_5$. The results of characteristic structure indicate that $Ag_4Bi_2O_5$ is evenly distributed in the MnO_2 material and affects the original structure of MnO_2. The electrochemical performances of the doped electrode in the alkaline electrolyte are measured by galvanostatic method and cyclic voltammetry tests. Results show that the doped electrode has excellent electrochemical properties and its discharge voltage is 50–100 mV higher than that of the traditional MnO_2 electrode. The doped electrode can offer a discharge specific capacity of 481 mAh g^{-1} at 120 mA g^{-1}. The cycling life of the doped electrode reaches up to 115 cycles, which is 3.4 times longer than that of electrolytic MnO_2 electrode at a high current density of 1000 mA g^{-1}. The effect of doping $Ag_4Bi_2O_5$ is much better than that of doping Bi_2O_3 or Ag_2O independently, which indicates that $Ag_4Bi_2O_5$ shows more superior electrochemical performance with the assistance of both Ag and Bi cations.

1. Introduction

The alkaline Zn/MnO_2 battery has occupied a dominant position in the civil battery field due to its reliable performance and convenience in use since it was commercialized [1–3]. With the rapid development of electronic digital products and the increasing consciousness of resource conservation, people now have paid more and more attention to the heavy load discharge performance and the rechargeability of the alkaline Zn/MnO_2 battery [4]. The property of MnO_2 cathode becomes a bottleneck that restricts the battery performance as compared with Zn anode which has good electrochemical performance [5,6]. Some new technologies such as ultra-thin steel shell and expanded graphite are used and the discharge capacity of the alkaline Zn/MnO_2 battery has been improved a lot. Many studies on the doping of Bi_2O_3 [7–10], PbO_2 [11], $PbTiO_3$ [12], $NaBiO_3$ [13–14] and other materials [15–23] into MnO_2 electrodes have been reported. Although the doping agent could further enhance the electrochemical performance of MnO_2, there are still many deficiencies in increasing power and prolonging service life. By comparison, $NaBiO_3$ has better doping effect, however, the Na cation is ineffective on improving the electrochemical performance of MnO_2. In view of the shortcoming of $NaBiO_3$, we introduce a new doping material, the derivates of sodium bismuthate—$Ag_4Bi_2O_5$, in which both bismuth and silver play the role of doping or assistance, and further improve the discharge capacity and cyclability of manganese dioxide. Although Jansen synthesized $Ag_4Bi_2O_5$ by solid state reaction of Ag_2O and Bi_2O_3 under an oxygen pressure of 10 MPa at a temperature of 200 °C [24–26], its electrochemical property and the doping effect on MnO_2 electrode have not been reported until now.

In this paper, the $Ag_4Bi_2O_5$ dopant was synthesized by precise control of precipitation reaction at low temperature of 45 °C and doped into the MnO_2 electrode. The characteristic structure of MnO_2 doped with nano $Ag_4Bi_2O_5$ was examined by means of X-ray powder diffraction (XRD) and energy-dispersive X-ray spectroscopy (EDS). The electrochemical performances and doping mechanism of the doped electrode were studied by galvanostatic method and cyclic voltammetry tests. The results show that the doped electrode provides long cycling life and high power.

2. Experimental

2.1. Synthesis of $Ag_4Bi_2O_5$-EMD

The $Ag_4Bi_2O_5$ was synthesized by precise control of precipitation reaction. 1.70 g $AgNO_3$ and 2.43 g Bi $(NO_3)_3{\cdot}5H_2O$ were dissolved in 50 mL 0.5 M HNO_3 (solution A). 11.87 g KOH (95 wt.%) was dissolved in 50 mL deionized water (solution B). Under the condition of a constant temperature of 45 °C and a strong

* Corresponding author at: State Key Laboratory of Chemical Resource Engineering, Beijing University of Chemical Technology, Beijing 100029, China.
Tel.: +86 10 64449332; fax: +86 10 64449332.
** Corresponding author.
E-mail addresses: jqpan@mail.buct.edu.cn (J. Pan), sunyanzhi@sohu.com (Y. Sun).

0378-7753/$ – see front matter © 2011 Published by Elsevier B.V.
doi:10.1016/j.jpowsour.2011.10.061

agitating at 600 rpm, solution A was pumped into solution B by using a constant flow pump. The flux was 0.2 mL min^{-1}. The pH of solution kept 13.00 in the whole reaction process. When the reaction was finished, the solution was aged for 1 h to make sedimentation complete, followed by washing the precipitation product with deionized water until the filtrate to present neutral. Then the product was dried in vacuum at 60 °C for 2 h and the final sample was obtained. The reaction took place in accordance with:

$$4AgNO_3 + 2Bi(NO_3)_3 + 10KOH = Ag_4Bi_2O_5\downarrow + 10KNO_3 + 5H_2O$$

Electrolytic manganese dioxide (EMD) powders (Xiangtan Electrochemical Technology Stock Co., Ltd.) were doped with the above self-prepared nano $Ag_4Bi_2O_5$ powders at various ratio (wt.%). Both powders were well mixed until homogenization in an agate mortar for about 60 min. The prepared product was physically modified $Ag_4Bi_2O_5$-EMD. The pure EMD was used as contrast sample, which has a theoretical specific capacity of 308 mAh g^{-1} in regard to one-electron discharge step.

2.2. Morphological and structural characterization

The XRD patterns were collected by means of a Rigaku D/max2500VB2+/PCX diffractometer with a Cu anticathode (40 kV, 200 mA), a scan rate of 10° min^{-1} and a scan angle (2θ) from 10° to 90°. The morphology and granularity of $Ag_4Bi_2O_5$-EMD were examined by means of FSEM (Cambridge S250MK3) observation. The element analysis was performed using EDS.

2.3. Electrochemical measurements

80 mg $Ag_4Bi_2O_5$-EMD, 20 mg expansive graphite and 5% PTFE (60 wt.%) binder were mixed in an agate mortar for 30 min. The prepared product was rolled on a rolling machine to form membrane with thickness of 80 μm. Then the membrane was pressed on the nickel foam plate as working electrode. A pure nickel wire was used as counter electrode, a Zn/ZnO as reference electrode (−1.36 V Vs. Hg/HgO electrode) and 9 M KOH as electrolyte. The three-electrode battery system was aged for 3 h, the charge–discharge test and electrochemical properties test were carried out with a LAND CT2001A battery test system and a CSU300 electrochemical workstation, respectively.

3. Results and discussion

3.1. Surface morphology and structural characterization

Both pure EMD and the EMD doped with $Ag_4Bi_2O_5$ at different proportion (5%, 10%) were studied with XRD. The results are illustrated in Fig. 1. The EMD sample has four strong and wide peaks at 22.16°, 37.26°, 42.64° and 56.60°, corresponding to (1 1 0), (0 1 1), (2 2 0) and (2 2 1) line of the ramsdellite structure respectively. It can be seen that the doping of $Ag_4Bi_2O_5$ makes the sample present three new strong peaks at 31.07°, 31.8°, 37.5°, respectively and the peaks intensity are enhanced with increase in doping amount. These results indicate that the nano $Ag_4Bi_2O_5$ is doped into EMD, which obviously affects the crystal structure of EMD.

Fig. 2 is the FSEM images of pure EMD and the $Ag_4Bi_2O_5$-EMD with doping ratio of 10%. From the photo, we can see that the pure EMD particles show irregular shape with actual grain sizes of 8–20 μm. The surface of $Ag_4Bi_2O_5$-EMD sample is obviously covered by tiny powders (Fig. 2(b)), meaning that $Ag_4Bi_2O_5$ has equably dispersed on the surface of EMD.

The EDS analysis is performed in order to confirm that the sample is doped with Bi and Ag elements. Fig. 3(a) and (b) represents the EDS analysis diagrams of the EMD and $Ag_4Bi_2O_5$-EMD sample respectively. It can be seen that only Mn and O elements appear in the EDS sample in Fig. 3(a). By contrast, Fig. 3(b) shows that Mn, O, Bi and Ag elements appear simultaneously in the $Ag_4Bi_2O_5$-EMD sample, indicating that the EMD is evenly doped with $Ag_4Bi_2O_5$.

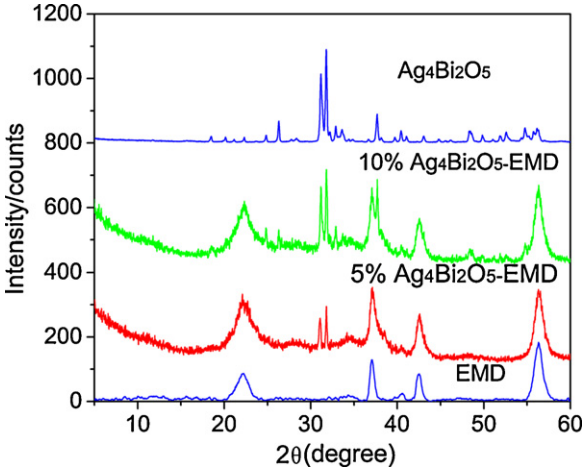

Fig. 1. The X-ray patterns of $Ag_4Bi_2O_5$, $Ag_4Bi_2O_5$-EMD and EMD powder samples.

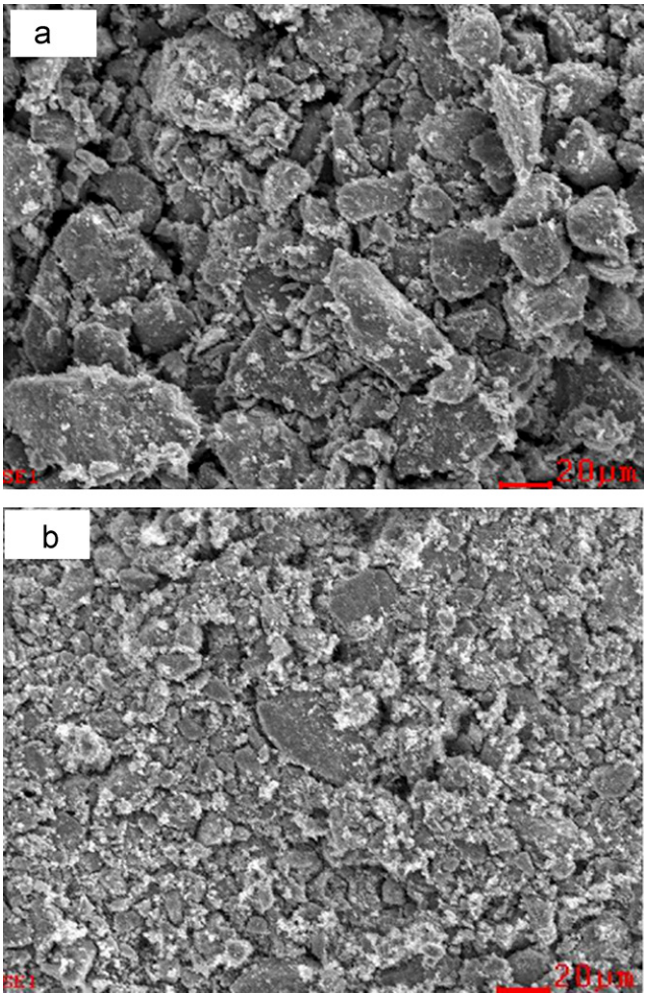

Fig. 2. The FSEM pictures of EMD (a) and $Ag_4Bi_2O_5$-EMD (b) samples.

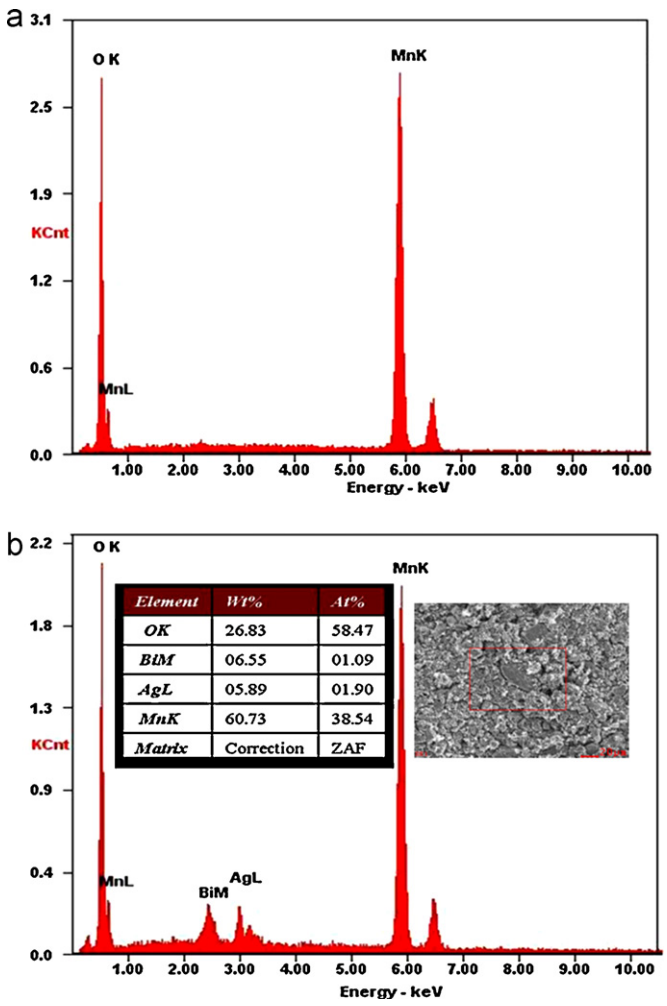

Fig. 3. The EDS analysis diagrams of EMD (a) and $Ag_4Bi_2O_5$-EMD (b) samples.

3.2. Electrochemical performance of $Ag_4Bi_2O_5$-EMD electrode

Fig. 4 shows discharge curves of EMD doped with $Ag_4Bi_2O_5$ of different proportion, and 10% Bi_2O_3 and 10% Ag_2O at a current density of 120 mA g^{-1}. It is obvious that the $Ag_4Bi_2O_5$ doped electrode has superior discharge performance than the pure EMD electrode, which reflects in two aspects: Firstly, the discharge voltage of the doped electrode is 50–100 mV higher than that of pure EMD electrode. Secondly, the discharge capacity of the doped electrode is obviously higher than that of pure EMD electrode. The doped electrode (doping ratio of 15%) offers a discharge specific capacity of 481 mAh g^{-1}, increasing by 59.2% as against the pure EMD (302 mAh g^{-1}) at a termination voltage of 0.6 V. The doping of $Ag_4Bi_2O_5$ contributes a lot to the second electronic capacity of MnO_2 in the discharge process, which leads to a great rise in capacity of the doped electrode. Generally, physical doping involves an optimal proportion range, so the relationship between doping ratio and discharge capacity is discussed. From the figure we can see that the increment of specific capacity is 468–360 mAh g^{-1} = 108 mAh g^{-1} when the doping amount increases from 5% to 10%. The increment is 481–468 mAh g^{-1} = 13 mAh g^{-1} when the doping amount increases form 10% to 15%. These calculation results show that the optimum doping proportion is 10%.

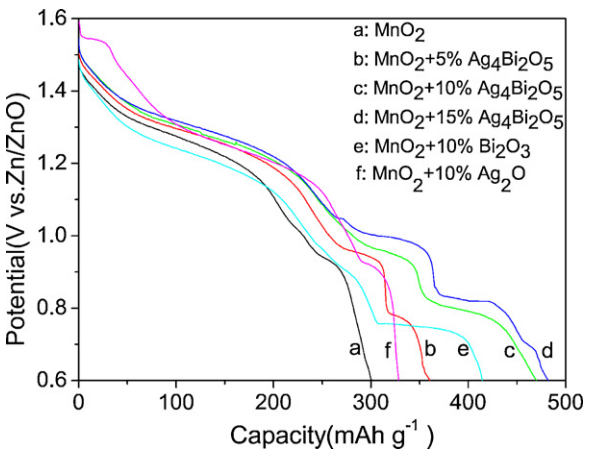

Fig. 4. Discharge curves of MnO_2 electrodes at 120 mA g^{-1} doped with different $Ag_4Bi_2O_5$ content (wt. %) (a) 0, (b) 5, (c) 10, (d) 15, (e) 10 wt.% Bi_2O_3 and (f) 10 wt.% Ag_2O.

It is also seen from Fig. 4 that there appears a small discharge platform at 1.54 V in the initial discharge stage (0–30.5 mAh g^{-1}) of MnO_2 doped with 10% Ag_2O. We speculate that this platform (23.1 mAh g^{-1}) on one hand mainly comes from the contribution of discharge capacity of 10% Ag_2O, on the other hand benefits from the increase in conductivity of MnO_2 electrode, which results from the reduction product of Ag_2O – the metallic Ag. This benefit of the increased conductivity of the doped cathode is also helpful to improve the whole discharge potential of MnO_2 electrode. However, the doping with Ag_2O cannot motivate the second electron discharge process of MnO_2 electrode and therefore the discharge capacity of Ag_2O-EMD is only 328 mAh g^{-1}, far lower than that of $Ag_4Bi_2O_5$-EMD (469 mAh g^{-1}) at a termination voltage of 0.6 V. For the electrode doped with 10% Bi_2O_3, it also expresses a certain extent of doping effect, but its discharge voltage and capacity (413 mAh g^{-1}) are all lower than that of $Ag_4Bi_2O_5$-EMD at the same doping level. The main difference is that a long discharge platform near l.0 V appears for the $Ag_4Bi_2O_5$ doped electrode while not appearing for Bi_2O_3. The measurement result shows that the discharge capacities at a cut-off voltage of 1.0 V for pure EMD electrode, the Bi_2O_3-EMD electrode and $Ag_4Bi_2O_5$-EMD electrode (doping ratio 10%) are 227, 236 and 281 mAh g^{-1}, respectively. These data indicate that doping of $Ag_4Bi_2O_5$ can improve the electrochemical properties of EMD at above 1.0 V, thus satisfy the demand of digital products. In addition, the discharge voltage of $Ag_4Bi_2O_5$-EMD electrode is 100 mV higher than that of Bi_2O_3-EMD electrode in the first half discharge process. The $Ag_4Bi_2O_5$-EMD electrode gives a discharge specific capacity of 469 mAh g^{-1}, which increases by 13.83% as compared with Bi_2O_3-EMD (412 mAh g^{-1}) at a termination voltage of 0.6 V. According to the above discussion, we think that the improvement of electrochemical performance of $Ag_4Bi_2O_5$-EMD electrode is probably due to the doping of Ag–Bi composite oxide which lacks electrons, beneficial to increasing vacancies in MnO_2 so as to increase the conductivity. Besides, cationic silver is a good conductor, of which doping increases the conductivity and reduces the cathodic polarization of the electrode, thus the discharge voltage and specific capacity of the doped electrode are further improved.

The cyclic voltammograms of pure EMD, $Ag_4Bi_2O_5$ and the $Ag_4Bi_2O_5$-EMD electrode in the deep discharge condition are shown in Fig. 5(a) and (b) respectively. The number in the figure represents cycle times. From Fig. 5(a), it can be seen that the reduction peaks area of pure EMD is less than oxidation peak area, the peak current successively decreases and reversibility decays quickly. However, Fig. 5(b) shows that the doped electrode has better reversibility than pure EMD. Firstly, the peak current of the doped electrode successively increase and the charge–discharge capacity keeps steady rise. Secondly, each peak potential and its corresponding reaction of the doped electrode are obviously

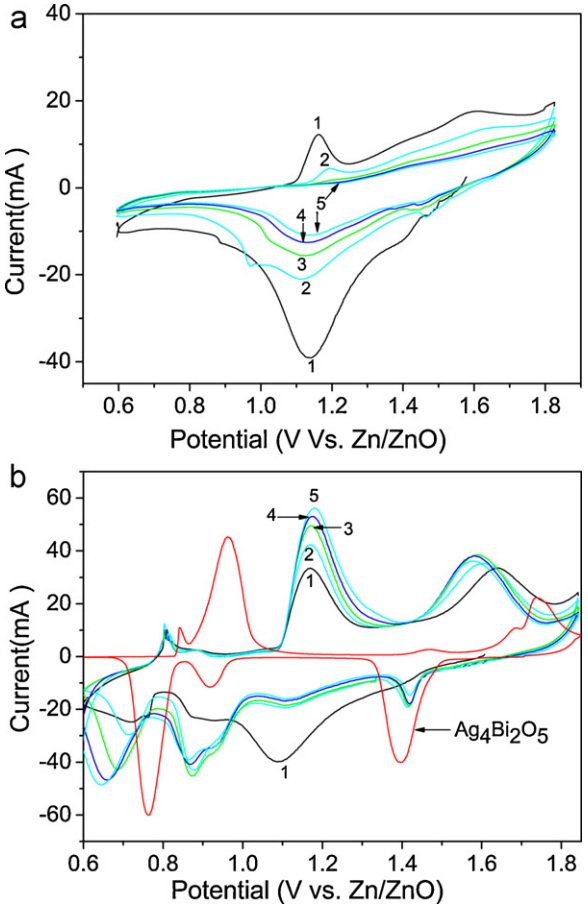

Fig. 5. Cyclic voltammetry curves of (a) EMD electrode, (b) $Ag_4Bi_2O_5$ (red line) and $Ag_4Bi_2O_5$-EMD electrode at a scan rate of 1 mV s^{-1}. (For interpretation of the references to color in this figure legend, the reader is referred to the web version of the article.)

different from those of pure EMD electrode. The good electrochemical performance of the doped electrode is due to quite different discharge mechanism of $Ag_4Bi_2O_5$ doping. From the CV curve of $Ag_4Bi_2O_5$ electrode, it can be seen that two high reduction peaks appear at 1.42 V and 0.76 V, respectively. The peak at 1.42 V may correspond to Ag(I) → Ag(0) [27]. Besides, the reduction potential of Bi(III) → Bi(0) in alkaline solution is −0.46 V vs. SHE, which is also equal to 0.80 V vs. Zn/ZnO reference electrode [28]. So we speculate that the reduction peak at 0.76 V is involved in Bi (III) → Bi(0). Corresponding to the reduction processes, two oxidation peaks at 0.96 V and 1.73 V are involved in Bi(0) → Bi(III) and Ag(0) → Ag(I), respectively. For the $Ag_4Bi_2O_5$-EMD electrode, there are four reduction peaks (Fig. 5(b)). According to the reduction peaks of $Ag_4Bi_2O_5$, we think that the first reduction peak appears at 1.4–1.45 V corresponds to the reaction Ag(I)Mn(IV) → Ag(0)Mn(IV). The second reduction peak appears at 1.1–1.2 V corresponds to the reaction Mn(IV) → Mn(III) [13]. The third reduction peak between 0.85 and 0.92 V is involved in Mn(III) → Mn(II) [13]. The fourth reduction peak near 0.75 V may correspond to the process of Bi(III) → Bi(0). Additionally, two obvious oxidation peaks appear in Fig. 5(b), the first oxidation peak at 1.15–1.25 V is very steep and peak current successively increases along with the increase in cycling times, which corresponds to Mn(II) → Mn(III) process. The second oxidation peak between 1.5 and 1.6 V may correspond to the reaction Mn(III)Ag(0) → Mn(IV)Ag(I). That is to say, the discharge mechanism of EMD has been changed completely by doping $Ag_4Bi_2O_5$.

Fig. 6 is the galvanostatic charge–discharge diagram of pure EMD and $Ag_4Bi_2O_5$-EMD electrodes in the first ten cycles. The

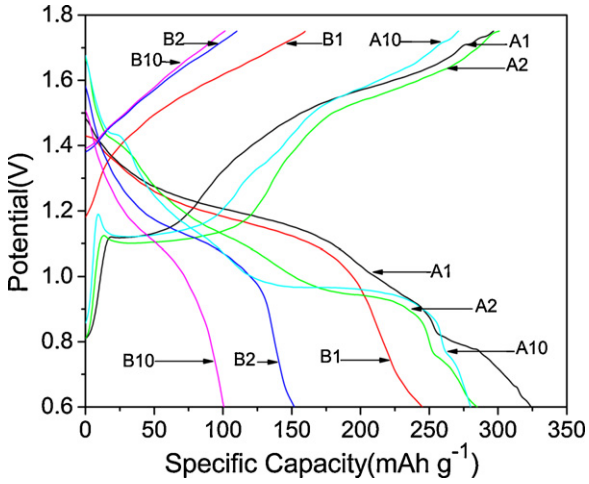

Fig. 6. The discharge/charge curves of $Ag_4Bi_2O_5$-EMD (A) and EMD (B) electrodes at a high current density of 1000 mA g^{-1}.

influence of nano $Ag_4Bi_2O_5$ on the specific capacity of EMD was studied through deep discharge of double electronic capacity with a cut-off voltage of 0.6 V. High charge–discharge rate was employed and a current density of 1000 mA g^{-1} was set. From the figure we can see that the doped electrode gives a specific capacity of 325 mAh g^{-1} in the first cycle, much higher than that of pure EMD (248 mAh g^{-1}). After 10 cycles, the doped electrode with a slow attenuation still offers 291 mAh g^{-1} of discharge specific capacity while pure EMD only gives 99 mAh g^{-1}. There is no obvious capacity decay of the doped electrode and the capacity of pure EMD reduces down by 39.9% as compared with the first cycle. This explains that the nano $Ag_4Bi_2O_5$ doping can improve the cycling property and charge–discharge capacity of EMD electrode.

Fig. 7 is the cycle capacity attenuation for EMD, Bi_2O_3-EMD, Ag_2O-EMD and $Ag_4Bi_2O_5$-EMD electrodes. The influence of different doping materials on the cycling life for EMD was studied through the single electron process with a cut-off voltage of 0.9 V. The electrodes underwent a high charge–discharge rate of 1000 mA g^{-1}. It is clearly illustrated by the graph that the charge–discharge specific capacity of $Ag_4Bi_2O_5$-EMD is much higher than that of the other three electrodes at the same cycle. Taking the first cycling capacity of EMD electrode (161.2 mAh g^{-1}) as starting line and provide that the service life of electrode reaches the end when its capacity reduces to 50%. Experimental results show that the pure EMD electrode, Ag_2O-EMD and Bi_2O_3-EMD electrode ends their life after 34, 27 and 76 cycles respectively. While

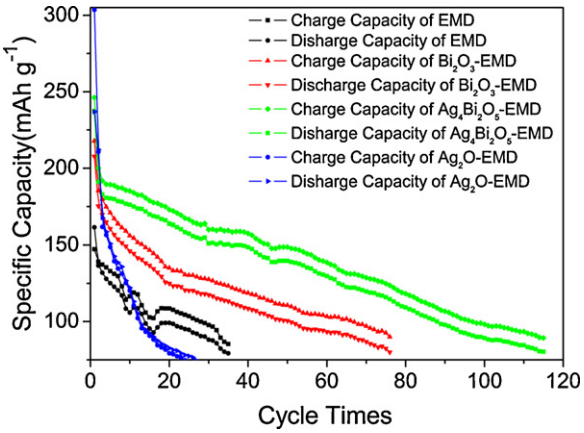

Fig. 7. Curves of cycling property of the EMD, Bi_2O_3-EMD, Ag_2O-EMD and $Ag_4Bi_2O_5$-EMD electrodes at a current density of 1000 mA g^{-1}.

the cycling life of $Ag_4Bi_2O_5$-EMD electrode reaches up to 115 cycles, which is 3.4 times longer than that of pure EMD electrode. It can also be seen from Fig. 7 that Ag_2O is beneficial to increasing the initial discharge capacity of the MnO_2 electrode, but has no effect on improving the cyclability of the electrode. Bi_2O_3 can increase the discharge capacity and improve the cycle life of the MnO_2 electrode to a certain extent by participating in the electrode reaction of manganese dioxide. However, $Ag_4Bi_2O_5$ not only significantly increases the discharge capacity of the MnO_2 electrode, but also increases the cycling life of the electrode from 76 cycles (doping with Bi_2O_3) to 115 cycles by combining the advantages of both silver oxide and Bi_2O_3. These data also indicate that doping nano $Ag_4Bi_2O_5$ can improve the cycling property of EMD electrode.

4. Conclusions

This article studies a novel MnO_2 cathode material doped with nano $Ag_4Bi_2O_5$. Results show that the $Ag_4Bi_2O_5$-EMD electrode has completely different charge–discharge mechanism from pure EMD. The discharge voltage is 50–100 mV higher than that of pure EMD and the doped electrode offers a discharge specific capacity of 481 mAh g^{-1} at 120 mA g^{-1}. The $Ag_4Bi_2O_5$-EMD electrode has excellent cycling property, of which cycling life is 3.4 times longer than that of EMD electrode at a high current density of 1000 mA g^{-1}.

Acknowledgements

This work was supported by Beijing Nova Program (2008B17), the Foundation of Excellent Doctoral Dissertation of Beijing City (YB20081001002) and National Natural Science Foundation of China (No. 21006003). The authors Prof. A. Manthiram and thank Prof. Xiaoguang Liu for the important discussions and modification of manuscript.

References

[1] D. Qu, J. Power Sources 102 (2001) 270.
[2] J. Tian, B. Liang, Y. Wang, S. Li, J. Electroanal. Chem. 526 (2002) 36.
[3] W. Jantscher, L. Binder, D.A. Fiedler, R. Andreaus, K. Kordesch, J. Power Sources 79 (1999) 9.
[4] M. Hibino, H. Kawaoka, H. Zhou, I. Honma, Electrochim. Acta 49 (2004) 5209.
[5] M.M. Sharma, B. Krishnan, S. Zachariah, C.U. Shah, J. Power Sources 79 (1999) 64.
[6] B. Sagdl, K. Micka, P. Krtil, Electrochim. Acta 40 (1995) 2005.
[7] V. Raghuveer, A. Manthiram, J. Power Sources 163 (2006) 598.
[8] M. Manickam, R.G.D. Mitchell, Electrochim. Acta 53 (2008) 6323.
[9] J. Yang, T.B. Atwater, J.J. Xua, J. Power Sources 139 (2005) 274.
[10] Kh.S. Abou-El-Sherbini, M.H. Askar, R. Schollhorn, Solid State Ionics 139 (2001) 121.
[11] Y.F. Yao, N. Gupta, H.S. Wroblowa, J. Electroanal. Chem. 223 (1987) 107.
[12] A.P. Barranco, F.C. Pinar, P. Martinez, E.T. Garcia, J. Eur. Ceram. Soc. 21 (2001) 523.
[13] J.Q. Pan, Y.Z. Sun, P.Y. Wan, Z.H. Wang, X.G. Liu, Electrochim. Acta 51 (2006) 3118.
[14] J.Q. Pan, Y.Z. Sun, P.Y. Wan, Z.H. Wang, M.H. Fan, J. Alloys Compd. 470 (2009) 75.
[15] V.K. Nartey, L. Binder, A. Huber, J. Power Sources 87 (2000) 205.
[16] M. Klob, D. Rahner, W. Plieth, J. Power Sources 69 (1997) 137.
[17] F. Zhang, K. Ngala, M.S. Whittingham, Electrochem. Commun. 2 (2000) 445.
[18] M. Manickam, R.G.D. Mitchell, K. Prince, Solid State Ionics 179 (2008) 355.
[19] S. Bodoardo, N. Penazzi, P. Spinelli, M. Arrabito, J. Power Sources 94 (2001) 194.
[20] J.L. Cao, L.T. Li, Z.L. Gui, Mater. Chem. Phys. 78 (2002) 546.
[21] R.K. Ghavami, Z. Rafiei, S.M. Tabatabaei, J. Power Sources 164 (2007) 934.
[22] M. Minakshia, M.G. Blackford, G.J. Thorogood, T.B. Issa, Electrochim. Acta 55 (2010) 1028.
[23] V. Raghuveer, A. Manthiram, Electrochem. Commun. 7 (2005) 1329.
[24] M. Jansen, S. Deibele, Z. Anorg. Allg. Chem. 622 (1996) 539.
[25] S. Deibele, M. Jansen, J. Solid State Chem. 147 (1999) 117.
[26] C.P.M. Oberndorfer, M. Jansen, Z. Anorg. Allg. Chem. 628 (2002) 1951.
[27] J.Q. Pan, Y.Z. Sun, Z.H. Wang, P.Y. Wan, X.G. Liu, M.H. Fan, J. Mater. Chem. 17 (2007) 4820.
[28] David R. Lide (Ed.), CRC Handbook of Chemistry and Physics, 90th ed., CRC Press/Taylor and Francis, Boca Raton, FL, 2010 (CD-ROM Version 2010).